ELSEVIER

Chemical Engineering Journal 70 (1998) 9–14

Chemical Engineering Journal

Liquid dispersion in gas–liquid–solid circulating fluidized beds

Shejiao Han [a,b], Jian Zhou [a], Yong Jin [a,*], Kai Chee Loh [b], Zhanwen Wang [a]

[a] *Department of Chemical Engineering, Tsinghua University, Beijing 100084, China*

[b] *Department of Chemical Engineering, National University of Singapore, 10 Kent Ridge Crescent, Singapore 119260, Singapore*

Received 24 February 1997; revised 1 November 1997; accepted 12 December 1997

Abstract

This paper presents a pioneering study of liquid dispersion in gas–liquid–solid circulating fluidized beds. The effects of the operating parameters, such as the gas velocity, liquid velocity and circulation flux of solids, on the liquid axial and radial dispersion coefficients were investigated. The experimental results indicated that the axial and radial liquid dispersion coefficients increased monotonically with increasing gas velocity; the axial liquid dispersion coefficients were insensitive to changes in the liquid velocity, but the radial liquid dispersion coefficients decreased with increasing liquid velocity; both the axial and radial liquid dispersion coefficients increased with increasing circulation flux of solids. Compared with traditional expanded beds, gas–liquid–solid circulating fluidized beds approach the ideal plug-flow reactor more closely.

Keywords: Gas–liquid–solid fluidization; Liquid velocity; Gas velocity; Circulation flux of solid

1. Introduction

Gas–liquid–solid fluidized beds have emerged as one of the most promising devices for three-phase operation. Such devices are of considerable industrial importance as shown by their wide application in chemical, petrochemical and biochemical processing. One mode of gas–liquid–solid fluidization is concurrent upward fluidization with liquid as the continuous phase. During recent decades, investigations on this mode have been focused mainly on expanded beds. For some gas–liquid–solid reaction systems in which the solids act as a catalyst, the solids are prone to deactivation arising from the deposition of by-products on the surface. The deactivated solid catalyst is usually regenerated externally. Reactivated solid catalyst can be re-fed into the bed by means of a downcomer to achieve a continuous operation. This is the origin of gas–liquid–solid circulating fluidized bed reactors [1–3].

Compared with traditional three-phase fluidized bed reactors, gas–liquid–solid circulating fluidized bed reactors have certain advantages: (1) the beds can be operated at high gas and liquid velocities, resulting in higher capacities; (2) more uniform distributions of bubble sizes and phase holdups can be achieved, providing better interfacial contact; (3) a high degree of turbulence can be realized, so that diffusional limitations can be minimized for some chemical reactions; (4) for exothermic reactions, particle circulation can move thermal energy away from the reactors, so that operation stability within reactors can be properly maintained. Consequently, processes with high efficiency and low energy consumption can be realized by means of three-phase circulating fluidized bed reactors.

Previous studies on three-phase reactors have been devoted to the liquid dispersion of conventional gas–liquid–solid fluidized beds [4], but little attention has been focused on gas–liquid–solid circulating fluidized beds. Investigations on liquid dispersion in three-phase circulating fluidized beds have not been reported.

In this study, liquid dispersion was studied in gas–liquid–solid circulating fluidized beds in terms of the effects of the following operating parameters: gas velocity, liquid velocity and circulation flux of solids.

2. Experimental details

A schematic diagram of the experimental apparatus (mainly consisting of a fluidized bed and a solid collector) is shown in Fig. 1. The Plexiglas column equipped with gas–liquid distributors is 3 m in height with an internal diameter of 0.140 m. The solid collector is composed of a liquid–solid separator, a cylinder for measuring solids and a solid tank.

Water is used as the liquid phase, and oil-free air as the gas phase. Glass beads with a diameter of 0.405 mm and a density

* Corresponding author.

1385-8947/98/$19.00
PII S1385-8947(98)00067-9

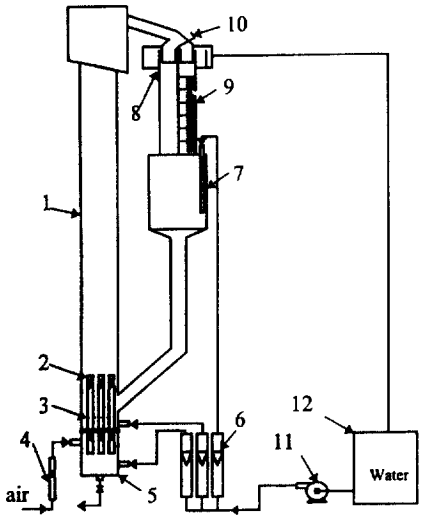

Fig. 1. Diagram of experimental set-up: 1, column; 2, gas–liquid distributor; 3, secondary liquid distributor; 4, gas flowmeter; 5, box; 6, liquid flowmeter; 7, particle tank; 8, liquid–solid separator; 9, particle measuring cylinder; 10, three-way valve; 11, liquid pump; 12, liquid reservoir.

of 2460 kg m^{-3} are used as the solid phase (the terminal velocity of a single glass particle in the gas–liquid medium is 5.4×10^{-2} m s^{-1}). In order to regulate the liquid and solid fluxes, water fed by a pump is divided into two streams: the main flow and secondary flow. The main flow, which has little influence on the rate of feed of solids, enters the bed from the bottom, while the secondary flow, which affects the rate of feed of solids, enters from the wall of the column. The distributor of the main liquid and gas flows is made up of seven perforated tubes located by a plate at the bottom of the column, and has an open rate of 15%. The secondary liquid flow is distributed by a porous plate with an open rate of 20%, situated between the entrances of the solid particles and secondary flow.

The water flow rates are measured by calibrated rotameters and regulated by globe valves. Oil-free compressed air is fed through a pressure regulator and a calibrated gas rotameter. The circulation flux of solids is determined by measuring the amount of particles collected in a measuring cylinder after closing the butterfly valve beneath the measuring cylinder.

3. Determination of the dispersion coefficients

The liquid dispersion coefficients were determined using the set-up shown in Fig. 2. The tracer (saturated potassium chloride solution) is contained in a reservoir connected to a nitrogen gas cylinder, which serves to maintain a constant pressure head above the tracer solution. By means of a solenoid valve controlled by an automatic timer, the tracer is injected into the centre of the column. A 0.02 s pulse of the tracer is injected using a syringe as a point source at the same velocity as the liquid interstitial velocity in the bed. The injection point is located 0.8 m above the bottom of the column to avoid the entrance effect.

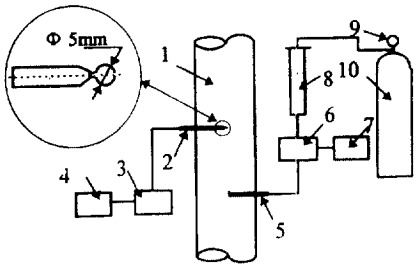

Fig. 2. Diagram of liquid dispersion measurement: 1, column; 2, conductivity probe; 3, conductivity meter; 4, personal computer; 5, tracer injector; 6, solenoid valve; 7, automatic timer; 8, saturated KCl tank; 9, pressure gauge; 10 nitrogen gas cylinder.

The concentration of tracer is detected by a conductivity probe located 0.2 m above the injection section point. This ensures good sensitivity for the determination of the dispersion coefficients. The probe is a pair of 0.5 mm diameter platinized wires. To obtain the radial tracer concentration profiles, the conductivity probe is installed at different radial positions along the cross-section. The conductivity gain obtained from the probe is converted to the tracer concentration using a calibrated relationship between the conductivity gain and KCl concentration.

4. Modelling of liquid dispersion coefficients

A two-dimensional plug-flow dispersion model is used to describe the liquid dispersion in gas–liquid–solid circulating fluidized beds. The following basic assumptions are made: (1) the liquid velocity distribution is uniform; (2) the bulk flow exists only in the axial direction; (3) the axial and radial dispersion coefficients are independent of position; (4) axisymmetric tracer concentration distribution exists.

The characteristics of liquid dispersion can be described by a coefficient of axial dispersion D_z and a coefficient of radial dispersion D_r. If the tracer is injected as a δ-function at the origin, the tracer concentration profiles can be evaluated by the dispersed plug-flow model as follows

$$D_z\frac{\partial^2 c}{\partial z^2}+\frac{D_r}{r}\frac{\partial}{\partial r}\left(r\frac{\partial c}{\partial r}\right)-\frac{U_l}{\varepsilon_l}\frac{\partial c}{\partial z}=\frac{\partial c}{\partial t} \quad (1)$$

with boundary conditions

$$r=R,\quad \frac{\partial c}{\partial r}=0 \quad (2)$$

$$r=0,\quad \frac{\partial c}{\partial r}=0 \quad (3)$$

$$z=-\infty,\quad c=0 \quad (4)$$

$$c(t,z,r)=c_0\quad \delta(t,z,r) \quad (5)$$

The distance L between the point of tracer injection and the measuring plane is positive in the direction of flow. The analytical solution of the equation is obtained as

$$\frac{c}{c_0}=\frac{e^{\varphi\xi}}{2\pi\sqrt{\pi\theta}}\sum_{n=0}^{\infty}\frac{J_0(\beta_n\rho)}{J_0^2(\beta_n)}\exp\left[-\frac{\xi^2}{4\theta}-(\varphi^2+\beta_n^2)\theta\right] \quad (6)$$

where β_n is the nth positive root of the Bessel function $J_1(\beta_n)$, and

$$\rho=\frac{r}{R},\quad \xi=\frac{z\sqrt{D_r}}{R\sqrt{D_z}},\quad \varphi=\frac{U_l R}{2\varepsilon_l\sqrt{D_z D_r}},\quad \theta=\frac{D_r t}{R^2} \quad (7)$$

5. Results and discussion

5.1. Characteristics of RTD

The experimental *RTD* curves in the gas–liquid–solid circulating fluidized bed are shown in Fig. 3. The *RTD* curves are found to be unimodal. Axial and radial liquid dispersion coefficients can be determined by fitting the experimental results of the temporal tracer concentration to the simulated profiles at different values of r/R. A two-dimensional, nonlinear, least-squares regression method is used for this purpose. A sensitivity analysis shows that the D_z values are sensitive to the shape of the *RTD* curves, and the D_r values are sensitive to the peak height of the *RTD* curves at different radial positions.

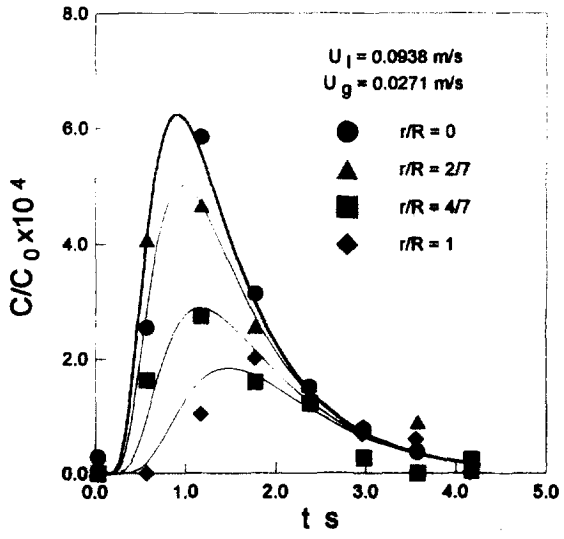

Fig. 3. Characteristics of *RTD* curves in the gas–liquid–solid circulating fluidized bed.

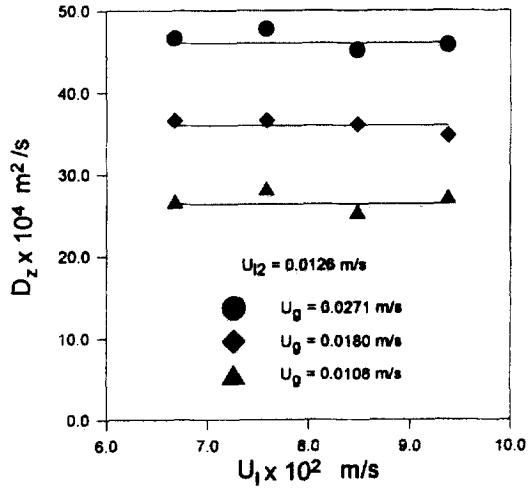

Fig. 4. Effect of liquid velocity on axial liquid dispersion coefficients.

5.2. Axial liquid dispersion coefficient

The variations in the axial liquid dispersion coefficient under different operating conditions are shown in Figs. 4–6. It can be seen that, in the gas–liquid–solid circulating fluidized bed, the axial liquid dispersion coefficients are independent of the liquid velocity, but increase monotonically with the increase in the gas velocity and circulation flux of solids.

It has been accepted that the axial movements of gas bubbles and wakes are the main causes of axial liquid dispersion in three-phase fluidized beds. Bubbles induce liquid mixing by the process of entrapping liquid into and shedding it from their wakes. The larger the wake, the greater this liquid mixing [4].

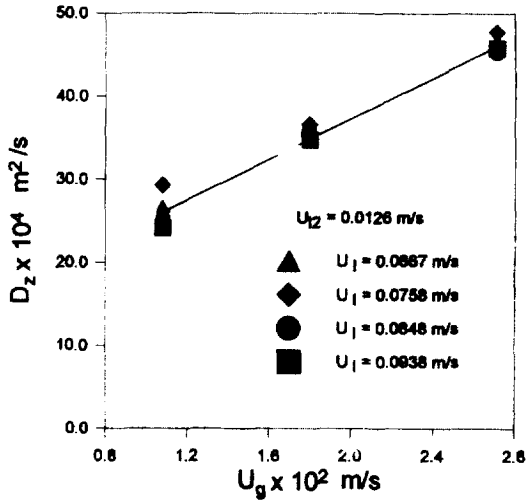

Fig. 5. Effect of gas velocity on axial liquid dispersion coefficients.

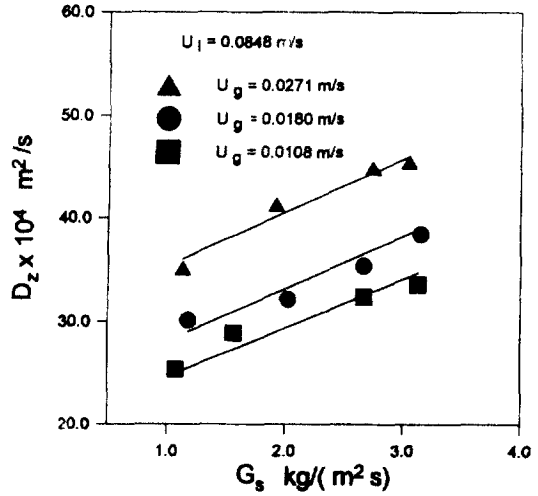

Fig. 6. Effect of solids circulation flux on axial liquid dispersion coefficients.

In gas–liquid–solid circulating fluidized beds, the bubble sizes are nearly independent of the liquid velocity because the bubbles are very small [2]. As a result, the liquid velocity has little effect on the axial liquid dispersion coefficient. In traditional fluidized beds, the effect of the liquid velocity on the axial liquid dispersion coefficient is dependent on many operating factors, such as the gas velocity, bed diameter, particle diameter and density, etc. In traditional fluidized beds of 3 mm and 6 mm particles, the experimental results reported [5] indicate that, within a particular operating range, the liquid velocity has little effect on the axial liquid dispersion coefficient. Kim et al. [5] proposed that this could be due to the break-up of some bubbles. Our experimental results are consistent with those reported by Kim et al. [5]. The increase in gas velocity results in increasing bubble sizes and wakes, and hence enhances the axial liquid dispersion. Bubble coalescence commonly occurs in fluidized beds of small particles, and this is attributed to the fact that the liquid–solid suspension acts as a pseudo-homogeneous medium of higher apparent viscosity [4]. An increase in the circulation flux of solids will cause an increase in the apparent liquid viscosity, resulting in an increase in the bubble size. Because an increase in bubble size leads to more vigorous liquid mixing, the axial liquid dispersion coefficient increases with increasing circulation flux of solids.

5.3. Radial liquid dispersion coefficient

The variations in the radial liquid dispersion coefficient under different operating conditions are shown in Figs. 7–9. In gas–liquid–solid three-phase circulating fluidized beds, there exists a more uniform distribution of the local liquid velocity in the radial direction with an increase in the liquid velocity [3]. Therefore, the velocity gradient of the liquid phase in the radial direction will be flattened, and the intercell recirculation of the liquid phase will be reduced, resulting in decreasing radial liquid dispersion coefficients with increasing liquid velocity, as shown in Fig. 7. As mentioned previously, an increase in the gas velocity and circulation flux of solids enhances bubble coalescence, thus promoting nonuniformity in the radial direction. Liquid dispersion will therefore be enhanced with an increase in the local liquid velocity gradient in the radial direction. As shown in Figs. 8 and 9, the radial liquid dispersion coefficients therefore increase with increasing gas velocity and circulation flux of solids.

5.4. Comparison of liquid dispersion coefficients

In the three-phase fluidized bed, the mechanism of liquid dispersion is complex. The liquid dispersion coefficients are affected by many factors, such as the velocities of the fluids, solid size, solid density, bed diameter and the physical properties of the continuous phase. It is difficult to compare the liquid dispersion coefficients obtained under different operating conditions; however, it can be seen from Table 1 that the axial liquid dispersion coefficients in circulating fluidized beds are much smaller than those in traditional beds, while the radial liquid dispersion coefficients are comparable in the range 0–10 $cm^2\ s^{-1}$. It can be expected that the liquid resi-

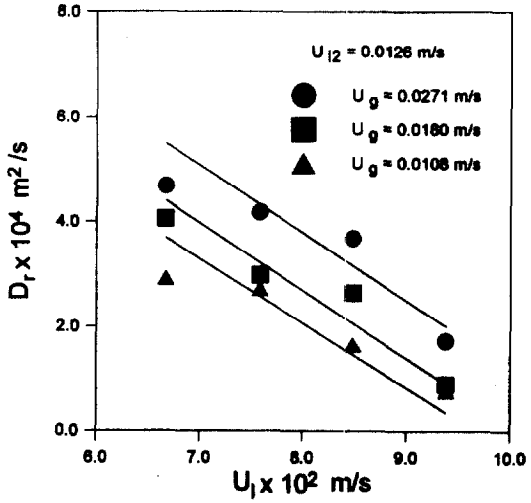

Fig. 7. Effect of liquid velocity on radial liquid dispersion coefficients.

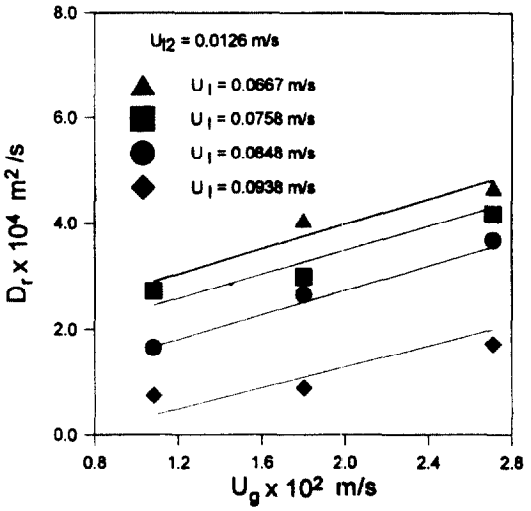

Fig. 8. Effect of gas velocity on radial liquid dispersion coefficients.

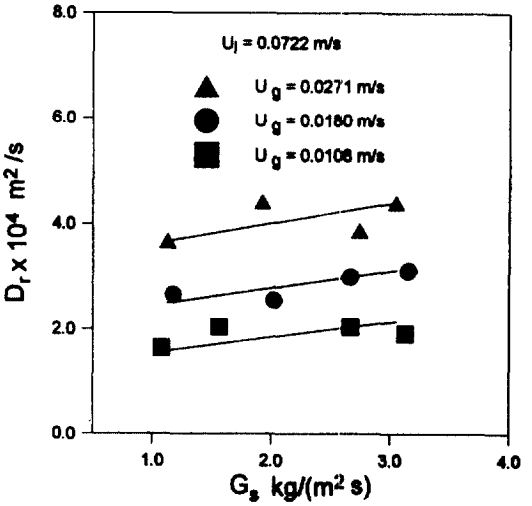

Fig. 9. Effect of circulation flux of solids on radial liquid dispersion coefficients.

Table 1
Comparison of liquid dispersion coefficients (experimental system: air–water–glass beads)

Ref.	$D_c\times10^3$ (m)	$d_p\times10^3$ (m)	$U_l\times10^3$ (m s^{-1})	$U_g\times10^3$ (m s^{-1})	$D_z\times10^4$ (m^2 s^{-1})	$D_r\times10^4$ (m^2 s^{-1})	Mode
El-Temtamy et al. [6,7]	50	0.45	11.5–32.5	13–50	40–100	0.5–5.0	Traditional three-phase fluidized bed
		0.96	25–70	13–50	25–100	0.5–5.0	
Kim and Kim [8]	145	1.7	20–130	0–120	10–150	–	Traditional three-phase fluidized bed
		3.0	20–130	0–120	20–250	–	
Kato et al. [9]	190	0.52	14–36	0–200	150–420	–	Traditional three-phase fluidized bed
	120		9–22		70–200	–	
Saberian-Broudjenni et al. [10]	52	1.4	30–90	10–135	50–200	–	Traditional three-phase fluidized bed
		2.1	30–90	10–135	30–150	–	
Han and Kim [11]	152	3.0	5–140	0–120	–	1–10	Traditional three-phase fluidized bed
Kang and Kim [12]	102	1.7	20–100	40	–	3–6	Traditional three-phase fluidized bed
Present paper	140	0.4	60–100	0–30	20–60	0.9–6.0	Three-phase circulating fluidized bed

dence time distribution in circulating fluidized beds will be closer to that of ideal plug flow.

5.5. Correlations

The experimental results shown in Figs. 3–9 indicate that the Peclet numbers can be represented as a function of the gas and liquid velocities, i.e., gas and liquid Reynolds numbers, and holdup of solids. Correlations for both axial and radial Peclet numbers were obtained by regressing all of the experimental data. The correlations obtained are

$$Pe_z = 3.2\times10^{-4}Re_l Re_g^{-0.5}(1-\varepsilon_s)^{2.8} \quad (8)$$

$$Pe_r = 6.7\times10^{-3}Re_l^{1.2}Re_g^{-0.8}(1-\varepsilon_s)^{0.4} \quad (9)$$

The average discrepancies between the calculated Pe_z and Pe_r and experimental Pe_z and Pe_r values were found to be less than 7.8% and 16.4%, respectively. The correlation for ε_s can be obtained from a previous paper [13].

6. Conclusions

Liquid dispersion has been investigated in gas–liquid–solid three-phase circulating fluidized beds for the first time. The experimental results are as follows.

(1) The axial liquid dispersion coefficients are insensitive to an increase in the liquid velocity, but increase with both increasing gas velocity and circulation flux of solids.

(2) The radial liquid dispersion coefficients decrease with increasing liquid velocity, but increase with both increasing gas velocity and circulation flux of solids.

(3) The axial liquid dispersion coefficients are much larger than the radial liquid dispersion coefficients; This indicates that liquid dispersion is dominated by axial liquid dispersion.

(4) The correlations for axial and radial liquid dispersion coefficients have been obtained.

(5) Compared with expanded beds, gas–liquid–solid three-phase risers approach the ideal plug-flow reactor more closely.

7. Nomenclature

c	concentration of KCl (mol m^{-3})
c_0	initial concentration of KCl (mol m^{-3})
d_p	diameter of particle (m)
D_c	diameter of column (m)
D_z	axial liquid dispersion coefficient (m^2 s^{-1})
D_r	radial liquid dispersion coefficient (m^2 s^{-1})
G_s	circulation flux of solids (kg m^{-2} s^{-1})
L	measuring distance (m)
Pe_z	Peclet number, $Pe_z=(LU_l)/D_z$
Pe_r	Peclet number, $Pe_r=(D_cU_l)/D_r$
Re_l	Reynolds number, $Re_l=(D_cU_l\rho_l)/\mu_l$
Re_g	Reynolds number, $Re_g=(D_cU_g\rho_g)/\mu_g$
U_g	superficial gas velocity (m s^{-1})
U_l	superficial liquid velocity (m s^{-1})
U_{l2}	secondary liquid velocity (m s^{-1})
U_t	terminal settling velocity of particle (m s^{-1})

Greek letters

β_n	the nth positive root for the Bessel function $J_1(\beta_n)=0$
ε_l	liquid holdup
ε_s	solids holdup
θ	dimensionless time, $\theta=(D_r\cdot t)/(R^2)$
μ_g	gas viscosity (Pa s)
μ_l	liquid viscosity (Pa s)
ξ	dimensionless axial position, $\xi=(z\sqrt{D_r})/(R\sqrt{D_z})$
ρ_g	gas density (kg m^{-3})
ρ_l	liquid density (kg m^{-3})
φ	dimensionless liquid velocity, $\varphi=(U_lR)/(2\varepsilon_l\sqrt{D_zD_r})$

References

[1] W.G. Liang, Q.W. Wu, Z.Q. Yu, Y. Jin, H.T. Bi, AIChE J. 41 (1995) 267.
[2] W.G. Liang, Q.W. Wu, Z.Q. Yu, Y. Jin, Z.W. Wang, Can. J. Chem. Eng. 73 (1995) 656.

[3] D. Mitra-Majumdar, B. Farouk, Y.T. Shah, Hydrodynamic modeling of three-phase flows through a vertical column, HTD (Am. Soc. Mech. Eng.) Proc. ASME Heat Transfer Division, Vol. 1, 1995, p. 227.
[4] L.S. Fan, Gas–Liquid–Solid Fluidization Engineering, Butterworth, 1989.
[5] S.D. Kim, H.S. Kim, J.H. Han, Chem. Eng. Sci. 47 (1992) 3419.
[6] S.A. El-Temtamy, Y.O. El-Sharnoubi, M.M. El-Halwagi, Chem. Eng. J. 18 (1979) 151.
[7] S.A. El-Temtamy, Y.O. El-Sharnoubi, M.M. El-Halwagi, Chem. Eng. J. 18 (1979) 161.
[8] S.D. Kim, C.H. Kim, J. Chem. Eng. Jpn. 16 (1983) 172.
[9] Y. Kato, S. Morooka, M. Koyama, T. Kago, S. Yang, J. Chem. Eng. Jpn. 18 (1985) 313.
[10] M. Saberian-Broudjenni, W. Gabrail, S.D. Kim, Chem. Eng. J. 40 (1989) 83.
[11] J.H. Han, S.D. Kim, Chem. Eng. Commun. 94 (1990) 9.
[12] Y. Kang, S.D. Kim, Ind. Eng. Chem. Process Res. Dev. 25 (1986) 717.
[13] W.G. Liang, Z.Q. Yu, Y. Jin, Z.W. Wang, Q.W. Wu, Chem. Eng. J. 58 (1995) 259.